Impact of GOLD Retrieved Thermospheric Temperatures on a Whole Atmosphere Data Assimilation Model

F. I. Laskar[1], N. M. Pedatella[2,3], M. V. Codrescu[4], R. W. Eastes[1], J. S. Evans[5], A. G. Burns[2], W. McClintock[1]

[1]Laboratory for Atmospheric and Space Physics, University of Colorado, Boulder, CO, USA
[2]High Altitude Observatory, National Center for Atmospheric Research, Boulder, CO, USA
[3]COSMIC Program Office, University Center for Atmospheric Research, Boulder, CO, USA.
[4]Space Weather Prediction Center, NOAA, Boulder, CO, USA
[5]Computational Physics, Inc., Springfield, Virginia, USA

Key Points:

- Synthetic level 2 GOLD disk temperatures are assimilated and tested in WACCMX+DART
- GOLD temperature assimilation improves the thermospheric temperature rmse and bias by 5-20% and 71-94%
- DW1 and local diurnal tide are improved by about 7% and 17%, respectively at thermospheric altitudes.

Corresponding author: Fazlul I. Laskar, `Fazlul.Laskar@colorado.edu`

Abstract

The present investigation evaluates the assimilation of synthetic data which has properties similar to actual Global-scale Observations of the Limb and Disk (GOLD) level-2 (L2) and other conventional lower atmospheric observations. The lower atmospheric and GOLD L2 temperature (T_{disk}) are assimilated in the Whole Atmosphere Community Climate Model with thermosphere-ionosphere eXtension (WACCMX) using Data Assimilation Research Testbed (DART). It is found that inclusion of the GOLD T_{disk} improves the forecast root mean square error (RMSE) and bias by 5% and 71%. When compared to lower atmosphere only assimilation the improvements in RMSE and bias are 20% and 94%. An investigation of the global DW1 and local diurnal tidal characteristics shows that inclusion of the GOLD temperatures improves the DW1 by about 8% and diurnal tide by more than 17%. The percentage improvement in tides is higher at lower thermospheric altitudes. Considerable improvements in the model state are also seen at times and locations where there are no GOLD observations available. These results and the background data assimilation procedure are presented here, which demonstrates that GOLD thermospheric temperature is an excellent dataset which can be used for thermospheric assimilation studies and operational purposes.

Plain Language Summary

A perfect numerical model simulation of the Earth is the one that can reproduce the whole atmosphere-ionosphere-thermosphere (AIT) system at any point of time. With time, the numerical models are evolving and the simulation capabilities are enhanced with new understanding of the AIT system dynamics, but they are still far from perfect. On the other hand if one can measure any parameters or state of the AIT system at any point of time then the numerical models will be of no use. In the absence of both the above highly ambitious extreme possibilities, both the state of the art model capabilities and AIT measurements can be combined in a data assimilation framework to study the dynamics and to get a better understanding of AIT system. The present investigation evaluates GOLD mission level-2 disk temperatures and found that they can improve the thermospheric assimilation capability significantly.

1 Introduction

The upper atmosphere, above about 100 km, of the Earth is influenced by wave forcing from the lower atmosphere and by external solar and geomagnetic forcings. For a better understanding of the whole atmosphere comprising of atmosphere-ionosphere-thermoshere (AIT) system it is necessary to study and characterize the local and global variations. Ground based datasets have good local time coverage but they lack global coverage. While low-earth orbiting (LEO) satellite based measurements have good global coverage but they lack local time coverage. However, imaging measurements from a geostationary orbit can cover a great spatial and temporal window over a part of the globe. The recently launched Global-scale Observations of the Limb and Disk (GOLD) mission provides one such opportunity to image the Earth's thermosphere at an unprecedented spectral, spatial, and temporal resolution (Eastes et al., 2020; McClintock et al., 2020; Laskar et al., 2020). GOLD scans the Earth's disk from geostationary orbit for about 18.5 hours a day, from 0610 UT to 0040 UT. The daylight measurements of the nitrogen (N_2) Lyman-Birge-Hopfield (LBH) bands in far-ultra-violet (FUV) can be used to retrieve thermospheric temperature over about, at times, one fourth of the globe (Eastes et al., 2020). With the availability of such partly global thermospheric dataset and other local plus global observations at different altitudes of the atmosphere an investigation of the AIT system is warranted by re-analyzing all these measurements.

The primary measurements from GOLD mission are FUV emissions, which can be used in the data assimilation models (Cantrall et al., 2019). But in the present inves-

tigation the thermospheric temperatures that are retrieved from the N_2 LBH bands are assimilated. This is because the temperatures retrieved from GOLD LBH band emissions are validated regularly and such retrievals have a long history (Aksnes et al., 2006; Krywonos et al., 2012; Meier et al., 2015). Moreover, investigations from a forward modeling study showed that model underestimate the radiance compared to GOLD observations (Greer et al., 2020).

The thermosphere-ionosphere (TI) system can change very rapidly with the change of external forcings. Also the lower atmospheric wave forcings influence the TI system significantly. So, a whole AIT data assimilation would be of great resource for the investigation of TI system (Jackson et al., 2019). Most of the earlier assimilation systems assimilated the lower atmosphere (below ∼100 km) data (Pedatella et al., 2014; McCormack et al., 2017) or used thermosphere-ionosphere models having a lower boundary between 80 km and 100 km altitudes (M. V. Codrescu et al., 2004; Lee et al., 2012; Chartier et al., 2016; Chen et al., 2017; Rajesh et al., 2017; S. M. Codrescu et al., 2018; Sutton, 2018; Cantrall et al., 2019; He et al., 2019).

Assimilation experiments using whole atmosphere models have also been performed (Wang et al., 2011; Pedatella et al., 2018), but they assimilated only the lower and middle atmosphere observations from altitudes below about 100 km. The present investigation aims to evaluate the impact of GOLD mission level-2 thermospheric disk temperatures on a whole AIT data assimilation model, where both lower atmosphere and thermosphere data are assimilated.

2 Model, Data, and Methodology

The main objective of this study is to assimilate and assess the impact of the GOLD disk temperatures (T_{disk}) observations in a whole atmosphere model, for that we have used the Whole Atmosphere Community Climate Model with thermosphere-ionosphere eXtension (WACCMX). Data assimilation is implemented using the Data Assimilation Research Testbed (DART) ensemble Kalman filter. Details about the model and observations are given below.

2.1 WACCMX+DART

The recently developed WACCMX version 2.1 is a whole atmosphere general circulation model extending from the surface to the upper thermosphere (500-700 km depending on solar activity) (Liu et al., 2018). WACCMX includes the chemical, dynamical, and physical processes that are necessary to model the lower, middle, and upper atmospheres. The thermosphere and ionosphere processes are similar to those in the NCAR Thermosphere-Ionosphere-Electrodynamics General Circulation Model (TIE-GCM), including the transport of O^+ and self-consistent electrodynamics as well as realistic solar and geomagnetic forcing. The model horizontal resolution is $1.9°\times2.5°$ in latitude and longitude, and the vertical resolution is 0.25 scale heights above ∼50 km.

To reproduce specific events in WACCMX it is necessary to constrain the model meteorology (i.e., dynamics). The data assimilation capability in WACCMX was initially implemented by Pedatella et al. (2018) using DART (Anderson et al., 2009), which uses the ensemble Kalman filter. But the earlier adoption was limited to assimilation of observations at altitudes below 100 km. In the present investigation the WACCMX+DART assimilation capability has been extended to thermosphere altitudes for the assimilation of GOLD L2 T_{disk}. As the thermospheric dynamics can change fast in response to changes in forcing conditions, we use 1 hour assimilation frequency.

An essential part of ensemble data assimilation is that the ensemble members should have sufficient spread. To increase the spread in the ensemble members we use variable

external forcing parameters with standard deviations of 15 sfu and 1 in F10.7 solar flux and Kp index over the ensemble members. For the assessment of the impact of assimilating GOLD T_{disk} data we run two Observing System Simulation Experiments (OSSEs); one with synthetic observations for altitudes below about 100 km, we call it lower atmosphere only (LA) and second one is with synthetic observations from lower atmosphere plus GOLD L2 T_{disk} (LA+GOLD) observations. These synthetic observations are generated based on a true or reference state from a free run of WACCMX. A random error is applied to the synthetic observations based on the errors in the actual observations.

For the present OSSEs the lower atmosphere observations include conventional meteorological observations (i.e., aircraft temperatures, radiosonde temperatures, and winds), Global Positioning System (GPS) radio occultation refractivity, and temperature observations from Thermosphere Ionosphere Mesosphere Energetics Dynamics (TIMED) satellite Sounding of the Atmosphere using Broadband Emission Radiometry (SABER) instrument and Aura Microwave Limb Sounder (MLS). The solar and geomagnetic forcing parameters for the true state is F10.7=76 sfu and Kp=0. While for the OSSEs the F10.7 has an ensemble mean value of 100 sfu and a spread of 15 sfu, resetting any F10.7 value less than 60 sfu to 60 sfu. Similarly, Kp index values have a mean of 0.33 with a spread of 1, but minimum Kp value was restricted to 0. Based on recommendations from previous studies (e.g., Pedatella et al., 2014, 2018) and to reduce the computational load we employ 40 member ensembles for both the OSSEs.

2.2 Assimilation of GOLD T_{disk} in WACCMX+DART

The daytime N_2 LBH bands can be used to retrieve lower thermospheric temperatures (Aksnes et al., 2006; Krywonos et al., 2012; Meier et al., 2015), which are publicly available in the GOLD web-page `https://gold.cs.ucf.edu/`. Figure 1 shows an example disk image of the retrieved temperatures from GOLD daytime disk observations (Figure 1a), their random uncertainty (Figure 1b), and a map of solar zenith angle variation over the disk (Figure 1c). A higher uncertainty in temperatures can be seen in the Northern hemisphere, which is due to low signal to noise ratio (SNR) corresponding to higher solar zenith angles (SZAs) measurements. Temperatures like these are retrieved from 1x1 pixel binned level 1C (L1C) LBH radiance data, so the noise level is high. In a future release the L1C data will be binned at 2x2 pixels to retrieve the disk temperatures, which will reduce the noise by about a factor of 7 (Eastes et al., 2020). Though the temperature data in 1x1 L1C pixel binning are noisy there are lot of geophysical variations in them, which are very clear in 2x2 L1C-pixel binning as can be seen in Eastes et al. (2020) or when some of the noisy data are filtered out (not shown here). So, to create a set of synthetic data for the current investigation, we have reduced the random uncertainty in the currently available operational data by 7 times.

The daytime N_2 LBH band emissions emanates primarily from the lower thermosphere. The altitude profiles of variation of 136.5 nm LBH band normalized contribution function for some representative solar zenith angles are shown in Figure 2(a). A contribution function provides information about the altitudes from where the emission emanated from. It can be noted that until about 55 degrees SZA the contribution function has nearly similar shape and the peak altitude varies by about 10 km. A plot of the 0° SZA contribution function and its mathematical function fit in $\log(p/p_\circ)$ coordinate, where p and $p_\circ$ are pressures at a given level and at the surface, respectively, is shown in Figure 2(b). As DART uses $\log(p/p_\circ)$ as vertical coordinate, we use such logarithmic scale in the forward operator calculations. The mathematical function used in the fit is a log normal function of the form:

$$CF_{fit} = (A/x)e^{\frac{-\{log_{10}(-x)-\mu\}^2}{2\sigma^2}} \quad (1)$$

Where, A, μ, σ are amplitude, mean and standard deviation of x, the actual contribution function. This function is used as the forward operator which translates the model

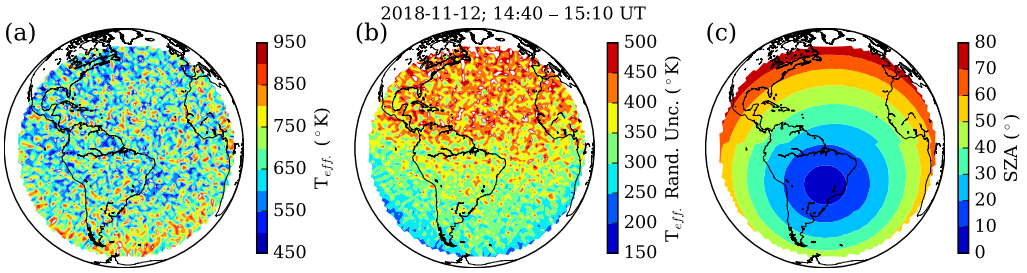

Figure 1. An example disk temperature image retrieved from GOLD daytime LBH disk observations (a), the random uncertainty (b), and a map of solar zenith angle variation over the disk are shown. Higher uncertainties in the Northern hemisphere are due to higher solar zenith angle and thus relatively lower signal to noise ratio measurements.

state to what would be observed by GOLD. Since GOLD observes airglow layer integrated emissions, which are used for the temperature retrieval, the forward operator weights the model temperature profiles to estimate a GOLD equivalent effective temperature.

2.3 Localization of the impact of GOLD observations

GOLD is capable of observing day-time Earth's disk temperatures centered over American longitudes, which are representative of the whole LBH emission layer as shown by the contribution functions in Figure 2. To avoid any spurious correlation at altitudes and locations far away from the observation point, the observations are localized in space so that there is no direct impact at far away locations. A plot of the variation of covariance vertical localization factor is shown in Figure 3. The peak of the vertical localization profile is close to the peak of the contribution function, which is about 160 km (or 10^{-5} hPa or -20 in log (p/p_0) coordinate). As the thermosphere maintains an isothermal state, a change in temperature at the peak altitude is expected to have a positive correlation at all altitudes in the thermosphere. Due to this characteristics of the thermosphere the localization function is chosen to be positive at upper thermosphere, even though the contribution function is near zero at those altitudes. The horizontal localization used is standard Gaspari-Cohn type (Gaspari & Cohn, 1999; Anderson & Lei, 2013) with a half width of 0.2 radians.

3 Results and Discussion

For the present OSSE investigation we test the assimilation of GOLD T_{disk} observations in WACCMX+DART for 9-13 November 2018, where the assimilation experiments started from 20 October 2018. Figure 4 shows an example of True (a), synthetic (c), forecast (b), and analysis (d) of GOLD disk temperatures on 13 November 2018 at 15 UT. It can be noted that the synthetic data used in these assimilations have spatial properties similar to those shown in Figure 1(a). The analysis states are obtained by assimilating the synthetic data in WACCMX+DART. The analysis state compares very well with the True state, which indicate that the data assimilation system performs well. Further diagnosis of the OSSEs are discussed below. It may be noted here that in the assimilation setup the T_{disk} observations only directly impact temperatures in WACCMX+DART.

Further diagnosis of the assimilation is performed by calculating root mean square error (RMSE) and bias between model (forecast and analysis) and T_{disk} observations. Figure 5 shows the variation of the RMSE (5a) and bias (5b) for the LA only analysis

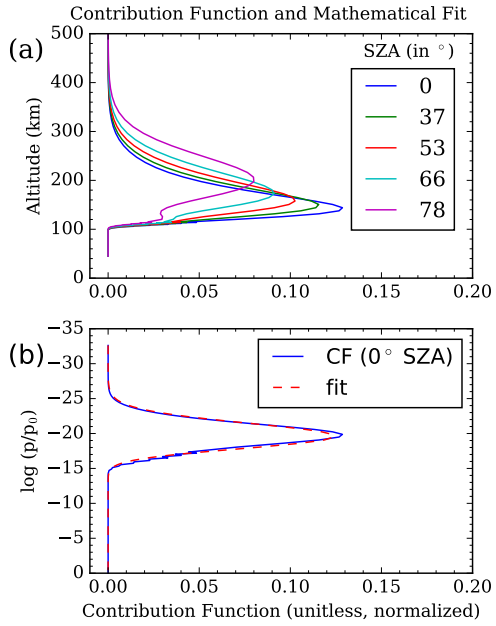

Figure 2. Variation of 136.5 nm LBH band contribution function for representative solar zenith angles (a). It can be noted that until about 60° SZA the contribution function has similar shape and does not differ much. A plot of the 0° SZA contribution function and its mathematical function fit in $\log(p/p_\circ)$ coordinate (b) that is used in the forward operator.

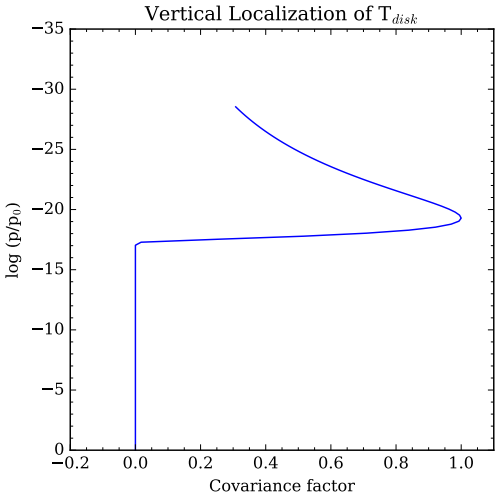

Figure 3. Variation of covariance localization factor with altitude. The peak of the vertical localization profile is close to the peak of the contribution function, which is about -20 (about 160 km or 10^{-5} hPa).

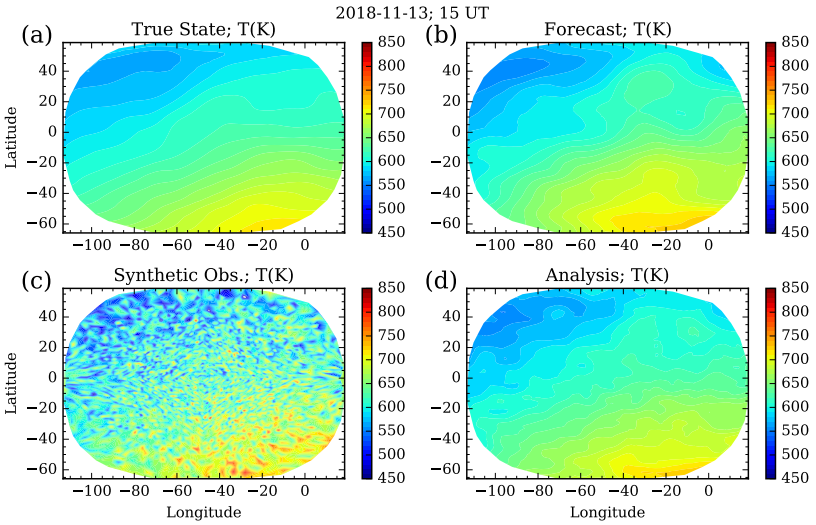

Figure 4. True (a), forecast (b), synthetic (c), and analysis (d) disk temperature states. It can be noted that the synthetic data used in this assimilation has spatial properties similar to those shown in Figure 1(a). The analysis state compares very well with the True state.

(LA anal.), LA+GOLD forecast (LA+GOLD fore.), and LA+GOLD analysis (LA+GOLD anal.). Significant improvement in LA+GOLD assimilated forecast RMSE and bias can be seen, which are about 5% and 71%. A dramatic improvement in LA only assimilation RMSE and bias are observed which are about 20% and 94%. It is also apparent in Figure 5 that the short-term forecast in the LA+GOLD experiment is improved relative to the LA experiment. This demonstrates the effectiveness of the assimilation, and shows that the assimilation of GOLD temperatures can improve short-term forecast of the thermosphere.

Figure 6 shows a comparison of the whole atmosphere temperature profiles from true state, LA only assimilation, and LA+GOLD assimilation for 14 UT (left column) and 18 UT (right column) at different locations inside the GOLD's field of view. Though there are differences between the true state and the analysis state in the LA+GOLD experiment, the differences are lower compared to the LA only experiment. It may be noted that the average solar forcing for the assimilation experiments is about 25 sfu higher compared to the true state solar forcing. Significant improvements are also observed (not shown here but another representation is shown later) at all hours from 7 -23 UT, where data are available from the GOLD disk observations. The zonal mean (ZM) temperature profiles (lower panels in Figure 6) also show significant improvement compared to LA only assimilation. These improvements in the analysis state suggests that GOLD T_{disk} improves the model state significantly.

The results in Figure 6 were for sample times and locations within the GOLD's observing temporal and spatial windows. Whereas, in Figure 7, we show a similar comparison as that in Figure 6 but at locations outside GOLD's field of view, to see its impact. Figure 7(a) and (b) show comparison at 2 UT and 15 UT and over (65°N, 60°W) where there are no or very little observations from GOLD. Even then one can note some improvement in the LA+GOLD analysis state compared to LA analysis. While in Figure 7(c) and (d) the same 2 UT and 15 UT are shown but at the other side of the hemisphere at (0°S, 120°E). As there are no observations from GOLD over those locations, the improvements compared to LA analysis is very small. This improvement in the LA+GOLD analysis outside the GOLD's field of view suggests that there are indirect improvement

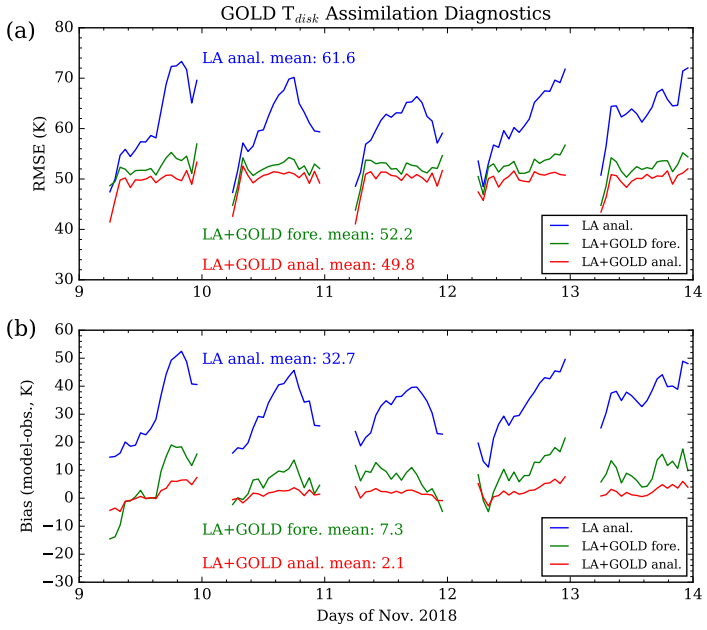

Figure 5. Diagnostics of the assimilation performed using lower atmosphere plus GOLD data are compared with lower atmosphere only assimilation. RMSE (a) and bias (b) for the LA analysis (LA anal.), LA+GOLD forecast (LA+GOLD fore.), and LA+GOLD analysis (LA+GOLD anal.). Significant improvement in LA+GOLD analysis RMSE and bias can be seen which are about 5% and 71%, compared to LA+GOLD forecast state. When compared to LA only assimilation the improvement in RMSE and bias are about 20% and 94%.

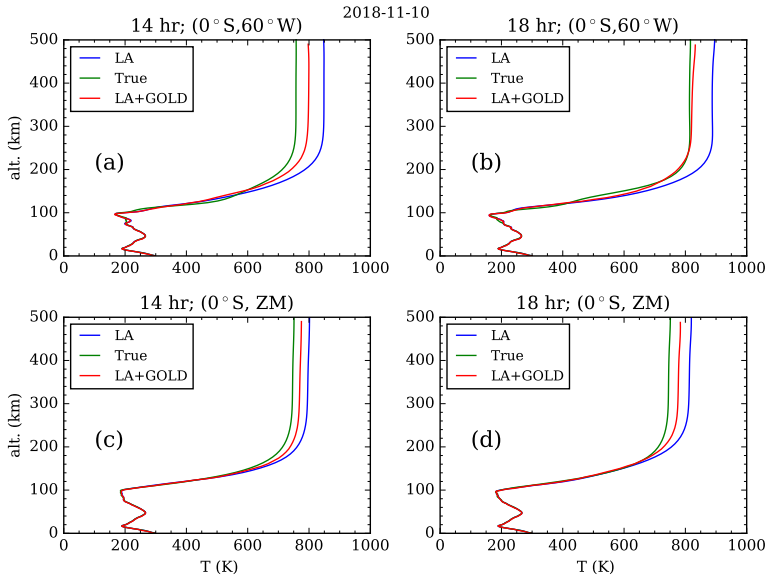

Figure 6. Comparison of the whole atmosphere temperature profiles from true state, lower atmosphere only assimilation (LA), and lower-atmosphere plus GOLD assimilation (LA+GOLD) for 14 UT (left column) and 18 UT (right column) at different locations inside the GOLD field of view. The zonal mean (ZM) in LA+GOLD also shows significant improvement compared to LA only assimilation.

in terms of the adjustment in the model forecast capability. Thus one can say that the assimilation of GOLD T_{disk} data improves the model state globally, but the impact is lower at locations and times outside GOLD's window of observations.

In Figure 8 we present a global picture of the impact of GOLD assimilation on model temperatures at a particular pressure level (7.3x10^{-7}hPa, about 194 km) but over the equator for the 5-days of OSSEs in November 2018. We show the difference between true state and the LA only assimilation (T_{LA}-T_{true}) in (a). While Figure 8(b) shows temperature difference between LA+GOLD experiment and true state ($T_{LA+GOLD}$-T_{true}) at that pressure. It can be seen that overall the differences are smaller in Figure 8(b) compared to Figure 8(a). Also, the $T_{LA+GOLD}$-T_{true} differences are very near to zero at second half of UT times of the day and within 110°W to 20°E longitudes through 0, where GOLD disk data are mostly available. There are some enhanced negative occurrences in ΔT within the 110°W to 20°E longitude (in Figure 8b), which are mostly in the night-sector where there are few or no observations from GOLD. One can see an enhanced region of temperature that is propagating with time along longitude, which is the signature of diurnal westward propagating wave number 1 (DW1) tide, characterization of such tides are given below.

We have observed above that DW1 like waves in temperatures are seen in Figure 8. Here we show the comparison of DW1 amplitudes between true, LA experiment, and LA+GOLD experiment in Figure 9(a). The DW1 amplitude is highest for the LA experiment and compared to it the LA+GOLD experiment DW1 has amplitudes closer to the true state. The percentage improvement in LA+GOLD experiment DW1 and percentage difference from true state are shown in Figure 9(b). The percentage improvements are higher than 7% at all the altitudes above about 130 km. Higher than 10% amplitudes are also observed in percentage improvement at altitudes below 150 km, which are mainly due to the lower values of true state DW1 tide in temperature. Though there

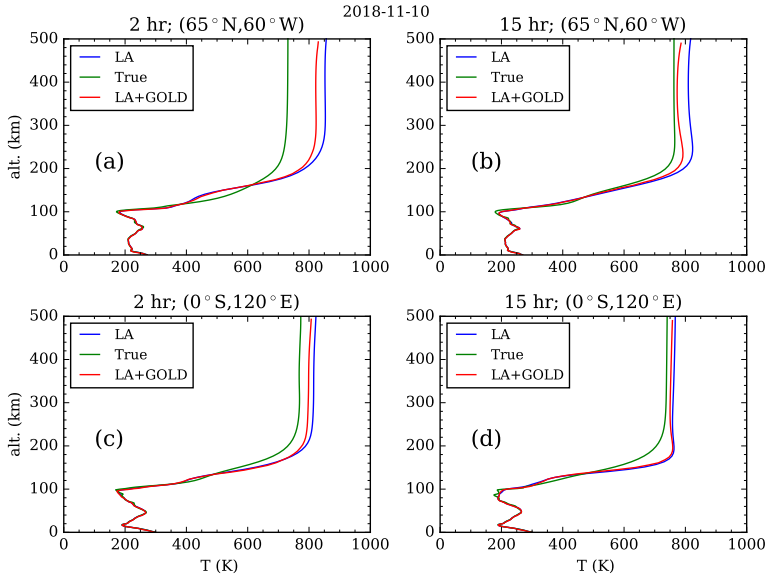

Figure 7. Comparison of the whole atmosphere temperature profiles between true state, lower atmosphere only assimilation (LA), and lower-atmosphere plus GOLD assimilation (LA+GOLD) for 2 UT (left column) and 14 UT (right column) at different locations outside the GOLD's field of view. Significant improvements are observed, even, at locations and times where there are no GOLD data.

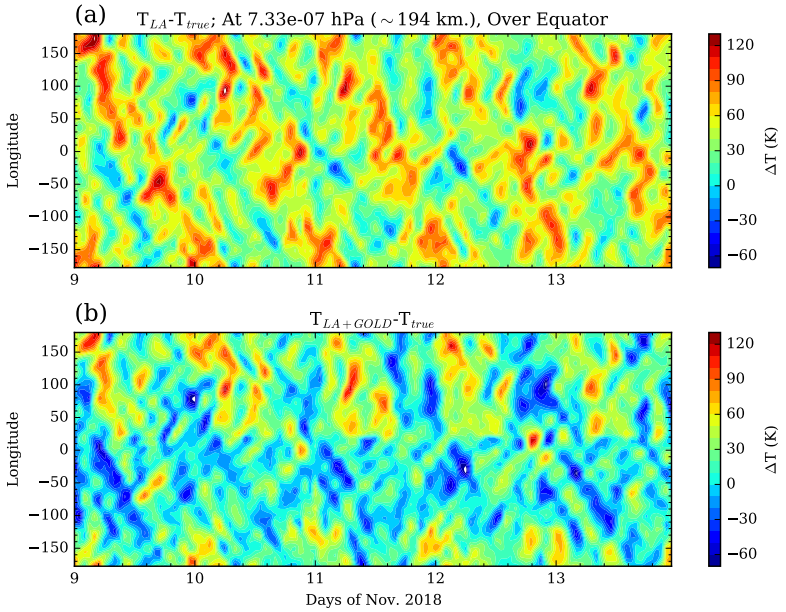

Figure 8. Longitudinal variation of the difference between true state and the lower atmosphere only assimilation (T_{LA}-T_{true}, in a) and true state and LA+GOLD assimilation ($T_{LA+GOLD}$-T_{true}, in b) are shown for the 5 days during November. It can be seen that the differences (in b) are very near zero at second half of UT days and at locations (110°W to 20°E, through 0°), where GOLD data are mostly available.

are more than 7% improvements in DW1 after assimilation of GOLD T_{disk}, there is still about 27% (about 10°K) difference between true and the GOLD assimilated DW1. This discrepancy could be attributed to GOLD only observing about one fourth of the globe for a portion of the day, so the improvement in the global DW1 tide is limited. But locally over American longitudes the improvement could be better which is discussed below.

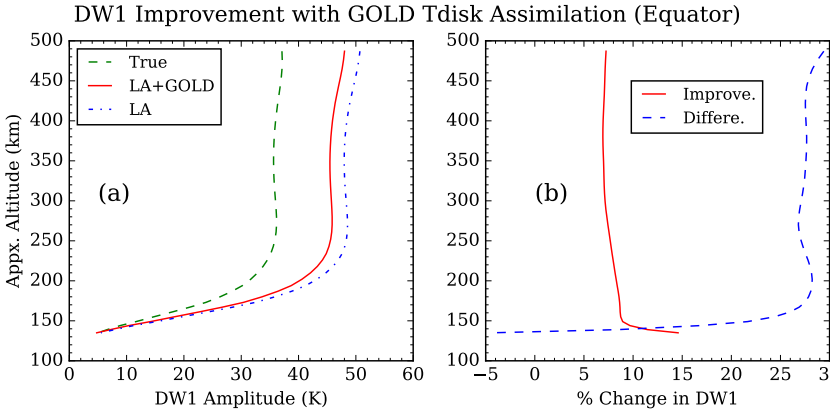

Figure 9. Improvement of DW1 amplitude as compared to LA assimilation experiment. Altitude variation of DW1 (a) of true (dashed), LA+GOLD (solid), and LA (dash-dotted) are shown. Percentage difference (dashed) and improvement (solid) in DW1 amplitudes (b) compared to true and lower atmosphere only assimilation DW1 amplitudes are also shown.

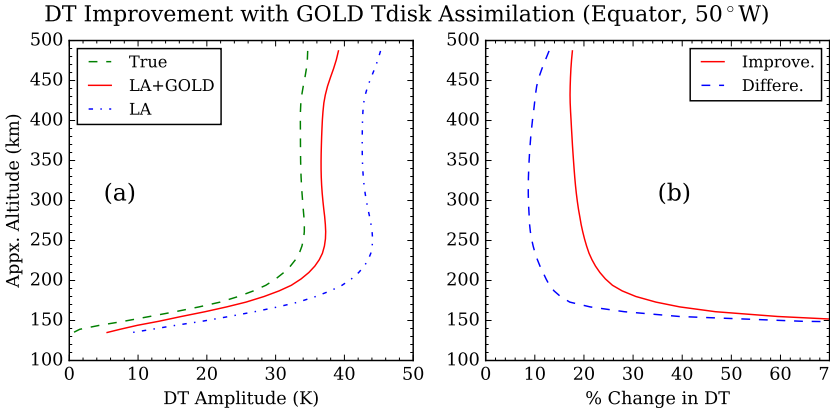

Figure 10. Improvement of local diurnal tidal (DT) amplitude as compared to LA only assimilation. Altitude variation of DT (a) of true (dashed), LA+GOLD (solid), and LA (dash-dotted) are shown. Percentage difference (dashed) and improvement (solid) in DT amplitudes (b) compared to true and lower atmosphere only assimilation DT amplitudes are also shown.

To investigate the local tides over the Americas we have done a similar analysis as that in Figure 9, but for the local diurnal tide (DT, at 0°, 50°W), which is shown in Figure 10. Here it can be seen that the LA+GOLD experiment DT amplitude profile is much closer to true state compared to LA experiment. Also, the improvements are more than 17% compared to LA assimilation and difference between true and LA+GOLD DT is

less than 10% at thermospheric levels. As the local tide estimation is affected by interaction between global and local components (Laskar et al., 2016) the discrepancies could be attributed to difference between global components of all the three states.

4 Conclusions

A set of synthetic observation from troposphere to thermosphere are used in this investigation to evaluate the impact of GOLD Level-2 disk temperature measurements to improve the thermospheric data assimilation and dynamics. Following are the salient findings of this investigation:

1. Assimilation of GOLD disk temperatures improves the themospheric assimilation over the GOLD field of view and also globally to some extent.
2. The model forecast RMSE and bias are improved by 5% and 71%, and the improvements are 20% and 94% when compared with lower atmosphere only assimilation. Thus, the inclusion of GOLD T_{disk} in the assimilation improves the short term forecast of the thermosphere.
3. The global diurnal tide of wavenumber 1 (DW1) and local diurnal tide over Americas improve by about 8% and by more than 17%, respectively upon assimilation of GOLD temperatures.
4. Though GOLD observations are available only during day-light hours, it improves the night time state too.

These results demonstrate that GOLD level 2 disk temperatures are an excellent set of observations, which will be of use in the future investigations of atmospheric coupling, dynamics, and operational use. As the GOLD T_{disk} assimilation improves thermosphere, the current investigation shows a promise towards better forecast capability of space weather.

Acknowledgments

This research was supported by NASA Contract 80GSFC18C0061 to the University of Colorado, Boulder. This material is also based upon work supported by the National Center for Atmospheric Research (NCAR), which is a major facility sponsored by the National Science Foundation under Cooperative Agreement No. 1852977. Computing and data storage resources, including the Cheyenne supercomputer (doi:10.5065/D6RX99HX), were provided by the Computational and Information Systems Laboratory (CISL) at NCAR. WACCMX is part of the Community Earth System Model (CESM) and the source code is available at `http://www.cesm.ucar.edu`. DART is available at `https://www.image.ucar.edu/DAReS/DART/`. The Level 2 data used in this study are available at the GOLD Science Data Center (`http://gold.cs.ucf.edu/search/`) and at NASA's Space Physics Data Facility (`https://spdf.gsfc.nasa.gov/pub/data/gold/`).

References

Aksnes, A., Eastes, R., Budzien, S., & Dymond, K. (2006). Neutral temperatures in the lower thermosphere from N_2 Lyman-Birge-Hopfield (LBH) band profiles. *Geophysical Research Letters*, *33*(15). doi: 10.1029/2006gl026255

Anderson, J., Hoar, T., Raeder, K., Liu, H., Collins, N., Torn, R., & Avellano, A. (2009, September). The data assimilation research testbed: A community facility. *Bulletin of the American Meteorological Society*, *90*(9), 1283–1296. doi: 10.1175/2009bams2618.1

Anderson, J., & Lei, L. (2013, October). Empirical localization of observation impact in ensemble kalman filters. *Monthly Weather Review*, *141*(11), 4140–4153. doi: 10.1175/mwr-d-12-00330.1

Cantrall, C. E., Matsuo, T., & Solomon, S. C. (2019, October). Upper atmosphere radiance data assimilation: A feasibility study for GOLD far ultraviolet observations. *Journal of Geophysical Research: Space Physics*, *124*(10), 8154–8164. doi: 10.1029/2019ja026910

Chartier, A. T., Matsuo, T., Anderson, J. L., Collins, N., Hoar, T. J., Lu, G., ... Bust, G. S. (2016, January). Ionospheric data assimilation and forecasting during storms. *Journal of Geophysical Research: Space Physics*, *121*(1), 764–778. doi: 10.1002/2014ja020799

Chen, C.-H., Lin, C., Chen, W.-H., & Matsuo, T. (2017, February). Modeling the ionospheric prereversal enhancement by using coupled thermosphere-ionosphere data assimilation. *Geophysical Research Letters*, *44*(4), 1652–1659. doi: 10.1002/2016gl071812

Codrescu, M. V., Fuller-Rowell, T. J., & Minter, C. F. (2004, November). An ensemble-type kalman filter for neutral thermospheric composition during geomagnetic storms. *Space Weather*, *2*(11), n/a–n/a. doi: 10.1029/2004sw000088

Codrescu, S. M., Codrescu, M. V., & Fedrizzi, M. (2018, January). An ensemble kalman filter for the thermosphere-ionosphere. *Space Weather*, *16*(1), 57–68. doi: 10.1002/2017sw001752

Eastes, R. W., McClintock, W. E., Burns, A. G., Anderson, D. N., Andersson, L., Aryal, S., ... Woods, T. N. (2020). Initial observations by the gold mission. *Journal of Geophysical Research: Space Physics*, *125*(7), e2020JA027823. doi: 10.1029/2020JA027823

Gaspari, G., & Cohn, S. E. (1999, January). Construction of correlation functions in two and three dimensions. *Quarterly Journal of the Royal Meteorological Society*, *125*(554), 723–757. doi: 10.1002/qj.49712555417

Greer, K. R., Eastes, R., Solomon, S., McClintock, W., Burns, A., & Rusch, D. (2020, June). Variations of lower thermospheric FUV emissions based on GOLD observations and GLOW modeling. *Journal of Geophysical Research: Space Physics*, *125*(6). doi: 10.1029/2020ja027810

He, J., Yue, X., Wang, W., & Wan, W. (2019, August). EnKF ionosphere and thermosphere data assimilation algorithm through a sparse matrix method. *Journal of Geophysical Research: Space Physics*, *124*(8), 7356–7365. doi: 10.1029/2019ja026554

Jackson, D. R., Fuller-Rowell, T. J., Griffin, D. J., Griffith, M. J., Kelly, C. W., Marsh, D. R., & Walach, M.-T. (2019, September). Future directions for whole atmosphere modeling: Developments in the context of space weather. *Space Weather*, *17*(9), 1342–1350. doi: 10.1029/2019sw002267

Krywonos, A., Murray, D. J., Eastes, R. W., Aksnes, A., Budzien, S. A., & Daniell, R. E. (2012, September). Remote sensing of neutral temperatures in the Earth's thermosphere using the Lyman-Birge-Hopfield bands of N_2: Comparisons with satellite drag data. *Journal of Geophysical Research: Space Physics*, *117*(A9). doi: 10.1029/2011ja017226

Laskar, F. I., Chau, J. L., Stober, G., Hoffmann, P., Hall, C. M., & Tsutsumi, M. (2016, May). Quasi-biennial oscillation modulation of the middle- and high-latitude mesospheric semidiurnal tides during august-september. *Journal of Geophysical Research: Space Physics*, *121*(5), 4869–4879. doi: 10.1002/2015ja022065

Laskar, F. I., Eastes, R. W., Martinis, C. R., Daniell, R. E., Pedatella, N. M., Burns, A. G., ... Codrescu, M. V. (2020, July). Early morning equatorial ionization anomaly from GOLD observations. *Journal of Geophysical Research: Space Physics*, *125*(7). doi: 10.1029/2019ja027487

Lee, I. T., Matsuo, T., Richmond, A. D., Liu, J. Y., Wang, W., Lin, C. H., ... Chen, M. Q. (2012, October). Assimilation of FORMOSAT-3/COSMIC electron density profiles into a coupled thermosphere/ionosphere model using

ensemble kalman filtering. *Journal of Geophysical Research: Space Physics*, *117*(A10), n/a–n/a. doi: 10.1029/2012ja017700

Liu, H.-L., Bardeen, C. G., Foster, B. T., Lauritzen, P., Liu, J., Lu, G., ... Wang, W. (2018). Development and validation of the whole atmosphere community climate model with thermosphere and ionosphere extension (waccm-x 2.0). *Journal of Advances in Modeling Earth Systems*, *10*(2), 381-402. doi: 10.1002/2017MS001232

McClintock, W. E., Eastes, R. W., Beland, S., Bryant, K. B., Burns, A. G., Correira, J., ... Veibel, V. (2020, May). Global-scale observations of the limb and disk mission implementation: 2. observations, data pipeline, and level 1 data products. *Journal of Geophysical Research: Space Physics*, *125*(5). doi: 10.1029/2020ja027809

McCormack, J., Hoppel, K., Kuhl, D., de Wit, R., Stober, G., Espy, P., ... Hibbins, R. (2017, February). Comparison of mesospheric winds from a high-altitude meteorological analysis system and meteor radar observations during the boreal winters of 2009–2010 and 2012–2013. *Journal of Atmospheric and Solar-Terrestrial Physics*, *154*, 132–166. doi: 10.1016/j.jastp.2016.12.007

Meier, R. R., Picone, J. M., Drob, D., Bishop, J., Emmert, J. T., Lean, J. L., ... Gibson, S. T. (2015, January). Remote sensing of earth's limb by TIMED/GUVI: Retrieval of thermospheric composition and temperature. *Earth and Space Science*, *2*(1), 1–37. doi: 10.1002/2014ea000035

Pedatella, N. M., Liu, H.-L., Marsh, D. R., Raeder, K., Anderson, J. L., Chau, J. L., ... Siddiqui, T. A. (2018). Analysis and hindcast experiments of the 2009 sudden stratospheric warming in WACCMX+DART. *J. Geophys. Res.: Space Physics*, *123*(4), 3131-3153. doi: 10.1002/2017JA025107

Pedatella, N. M., Raeder, K., Anderson, J. L., & Liu, H.-L. (2014). Ensemble data assimilation in the whole atmosphere community climate model. *J. Geophys. Res.: Atmospheres*, *119*(16), 9793–9809. doi: 10.1002/2014jd021776

Rajesh, P. K., Lin, C. H., Chen, C. H., Lin, J. T., Matsuo, T., Chou, M. Y., ... You, C. F. (2017, September). Equatorial plasma bubble generation inhibition during 2015 st. patrick's day storm. *Space Weather*, *15*(9), 1141–1150. doi: 10.1002/2017sw001641

Sutton, E. K. (2018, June). A new method of physics-based data assimilation for the quiet and disturbed thermosphere. *Space Weather*, *16*(6), 736–753. doi: 10.1002/2017sw001785

Wang, H., Fuller-Rowell, T. J., Akmaev, R. A., Hu, M., Kleist, D. T., & Iredell, M. D. (2011, December). First simulations with a whole atmosphere data assimilation and forecast system: The january 2009 major sudden stratospheric warming. *Journal of Geophysical Research: Space Physics*, *116*(A12), n/a–n/a. doi: 10.1029/2011ja017081